Applied Science and Innovative Research
ISSN 2474-4972 (Print) ISSN 2474-4980 (Online)
Vol. 1, No. 1, 2017
www.scholink.org/ojs/index.php/asir

Nanoscale Nucleation and Growth of Non-Stoichiometric V-Shaped InP Defect in Heterogeneous InGaAsP/InP Array

Jack Jia-Sheng Huang[1,2*], Chung Shyu[2], Yu-Heng Jan[1,2], Willy Lin[2], YiJu Chen[2], Ehsin Chen[2], ShinYi Shen[2], C. J. Ni[2], S. C. Huang[2], J. L. Hsieh[2] & Emin Chou[2]

[1] Source Photonics, West Hills, CA, USA

[2] Source Photonics, Science-Based Industrial Park, Hsinchu, Taiwan, R.O.C.

[*] Jack Jia-Sheng Huang, E-mail: jack.huang@sourcephotonics.com

Received: May 10, 2017 Accepted: May 18, 2017 Online Published: May 25, 2017

doi:10.22158/asir.v1n1p69 URL: http://dx.doi.org/10.22158/asir.v1n1p69

Abstract

Nanotechnology is a broad field that involves the manipulation of atoms and molecules. For nanophotonics, defect formation in nanostructured compound semiconductor system is of great technological interest. In this paper, we study the nanoscale nucleation and growth of V-shaped defect in the heterogeneous InGaAsP/InP array. We have observed that the nucleation originated from the phosphorus-deficient disordering that was likely induced by reactive ion etching. During the nucleation, the phosphorus-deficient $In_{1+x}P_{1-x}$ compound was developed at the trench. The triangular nano-precipitates of $In_{1+x}P_{1-x}$ with sizes of 20-30nm were formed. The ratio of In to P in the non-stoichiometric compound was higher in the upper portion of the V-defect, likely due to antisite defect mechanism. During the defect growth process, the phosphorus-deficient nucleation site expanded to form open, inverted pyramid with sidewalls following the crystallographic planes.

Keywords

nanotechnology, nanophotonics, semiconductor, defects, V-shaped defects, heterogeneous interface, reactive ion etching, surface energy

1. Introduction

Nanotechnology involves the study and application of extremely small things, typically in the range of 1 to 100 nanometers (Drexler, 1986; Saini et al., 2010; Regan et al., 2005; Narayan et al., 2004; Paull & Lyons, 2008; Dregely et al., 2011). The essential core of nanotechnology is the manipulation of atoms and molecules. The ideas and concepts behind nanotechnology originated from the Nobel laureate physicist Richard P. Feynman at California Institute of Technology (Feynman, 1992). On December 29, 1959, he delivered a talk entitled “There’s plenty of room at the bottom” that famously predicted that nanoscale matter could be squeezed on the head of a pin. Feynman discussed about manipulating and

controlling things on a small scale.

Today, nanophotonics have been increasingly studied in academia and industry (Bowers et al., 2010; Duan et al., 2003; Gilfert et al., 2010; Duan et al., 2001) due to their wide ranges of communication applications. The nanoscale photonics devices not only are small in dimensions, but also exhibit novel properties beyond imagination. For example, plasmonic nanowire lasers have been demonstrated to show low threshold current, high power and fast modulation (Sidiropoulos et al., 2014).

Defect engineering is an important subject for the practical applications of nanotechnology. Defects in various nanostructured systems such as carbon nanotubes (Fan et al., 2005; Charlier, 2002; Collins, 2009) and semiconductor nanowires (Korgel, 2006; Tham et al., 2006; Wang, 2006) have been studied in the past. For nanophotonics, defect formation in Light Emitting Diode (LED) or Laser Diode (LD) would be of practical interest. For the LED, it was reported that the V-shaped pits were formed in InGaN quantum wells (Chen et al., 1998; Wu et al., 1998).

In this paper, we study the V-shaped defect formation mechanism at the InP/InGaAsP system that is suitable for optical communication applications. We will reveal the nucleation process of the InP defect in the heterogeneous arrays. We will also discuss the defect growth mechanism of phosphorus-deficient InP compound induced by the heterogeneous nucleation.

2. Method

Figure 1 shows the fabrication schematic of the nanoscale heterogeneous InGaAsP/InP array. First, an InP buffer, an InGaAsP, and an InP cap layers were grown by Metal Organic Chemical Vapor Deposition (MOCVD) on an (001) InP substrate, as shown in Figure 1 (a). The InP cap was grown to protect the InGaAsP layer. Next, the Photoresist (PR) was deposited and lithography-exposed to form the soft mask on top of the InGaAsP and InP cap layers. After development, the width of each PR mask was 100 nm with a spacing of 100 nm between each PR, as shown in Figure 1 (b). Third, Reactive Ion Etching (RIE) based on BCl_3 and Ar gases was used to etch the InGaAsP/InP to form InGaAsP/InP nano-heterogeneous array, as shown in Figure 1 (c). Finally, the InP regrowth layer was overgrown to cover the InGaAsP/InP heterogeneous structure, shown in Figure 1 (d).

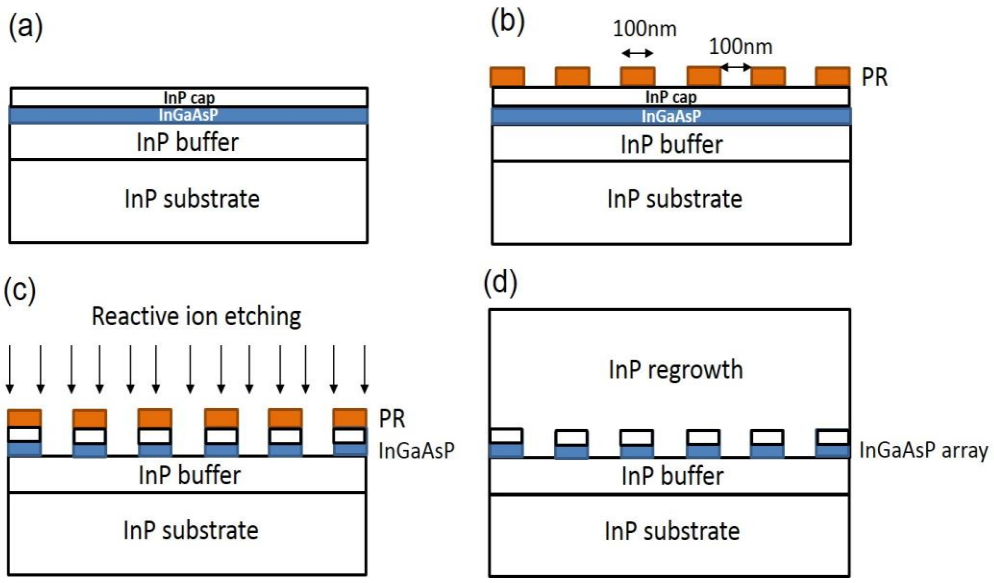

Figure 1. Fabrication Schematic of Nanoscale Heterogeneous InGaAsP/InP Array. (a) InP Buffer/InGaAsP/InP Cap Layers were Grown by MOCVD, (b) Photoresist Pattern was Formed, (c) RIE was Used to Form the InGaAsP/InP Nano-Heterogeneous Array, and (d) InP Regrowth Layer was Overgrown

To study the nanoscale defect formation, cross-sectional samples were prepared in a FEI Talos F200X Focused Ion Beam (FIB) system using the lift-out technique (Giannuzzi et al., 2010). The FIB samples were examined by high-resolution Transmission Electron Microscopy (TEM). The TEM accelerated at 200kV allowed rapid inspection of small features. The image was based on secondary electron signal, and the chemical element analysis was done by Energy Dispersive Spectroscopy (EDS) (Huang et al., 2002; Giannuzzi et al., 1997).

3. Result

Figure 2 shows the cross-sectional TEM bright-field image of the nano-heterogeneous InGaAsP/InP array. The InGaAsP array appeared dark in the TEM, while the InP buffer and InP regrowth appeared white. It was noted that a defect of inverted pyramid-shape (appeared light dark in the TEM image) was formed at the groove of the InP between the heterogeneous InGaAsP/InP arrays. Such pyramid-shaped defect was previously reported in InGaN material system, called V-pits (Chen et al., 1998; Kim et al, 1998) or V-defects (Wu et al., 1998; Sharma et al., 2000). The V-shaped defect expanded in the top InP regrowth layer. Another interesting finding was the formation of nano-precipitates, in adjacent to the InP cap. The size of nano-precipitates ranged from 20nm to 30nm.

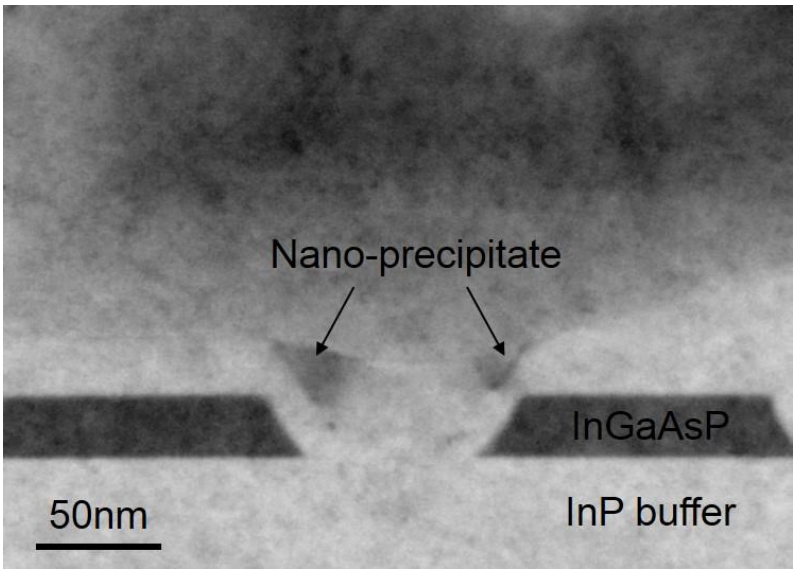

Figure 2. The Morphology of V-Defect Near the Heterogeneous InGaAsP/InP Array

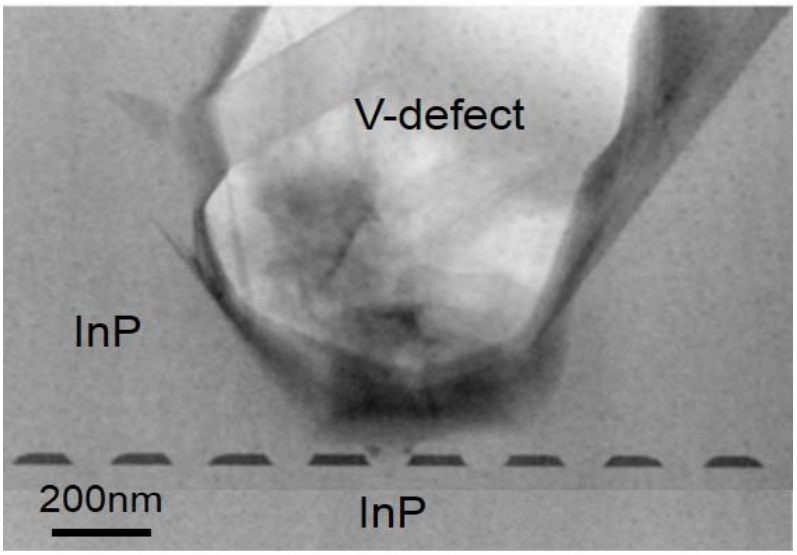

Figure 3. The Morphology of V-Defect Showing the Defect Growth in the InP Regrowth Layer. The Tip of the V-Defect was Located Near the Trench between the InGaAsP/InP Heterogeneous Arrays

Figure 3 shows the cross-sectional TEM image of the entire V-shaped defect that originated from the groove region and continued to propagate into the InP regrowth layer. The V-shaped defect grew in size as it approached the top surface. The sidewall boundaries were likely following the crystallographic planes (Chen et al., 1998; Wu et al., 1998).

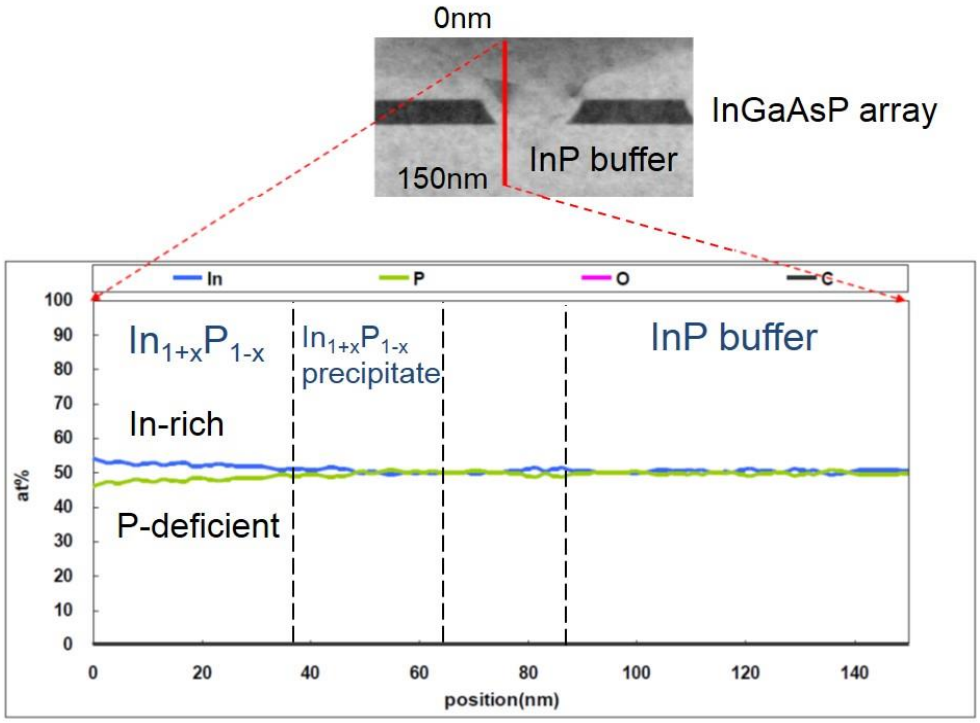

Figure 4. EDS Linescan at the Bottom of V-Defect Showing the InP Defect above and Near the Nano-Precipitate was Phosphorus-Deficient and Indium-Rich ($In_{1+x}P_{1-x}$)

In order to understand the formation mechanism of the V-shaped defect, we conducted EDS linescans across different parts of the V-defect to study the chemical composition and stoichiometry. Figure 4 shows the EDS linescan near the bottom of the V-defect. The linescan started from the top to the bottom across the depth of 150nm. The top layer of about 38nm marked the region above the nano-precipitate. The EDS linescan indicated that the region above the nano-precipitate was phosphorus-deficient and indium-rich ($In_{1+x}P_{1-x}$). The phosphorus-deficient phase further extended into the nano-precipitate. The non-stoichiometric compound was likely related to the antisite defect mechanism (Mattila & Nieminen, 1995; Seitsonen et al., 1994). Another intriguing observation was the compositional gradient in the non-stoichiometry between the In and P. As the linescan moved deeper from the surface, the ratio of In to P was decreasing. Below the nano-precipitate, the ratio of In to P approached to 1, the same stoichiometric compound as the InP buffer and cap layers.

Figure 5 shows the EDS linescan at the upper portion of V-defect after the growth process. Near the top of the V-defect, the non-stoichiometry was most pronounced, and the EDS indicated that the compound was $In_{0.6}P_{0.4}$. As the linescan moved deeper from the surface, the ratio of In to P was decreasing. For example, the composition of the non-stoichiometric compound was $In_{0.55}P_{0.45}$ at the the linescan depth of 100nm.

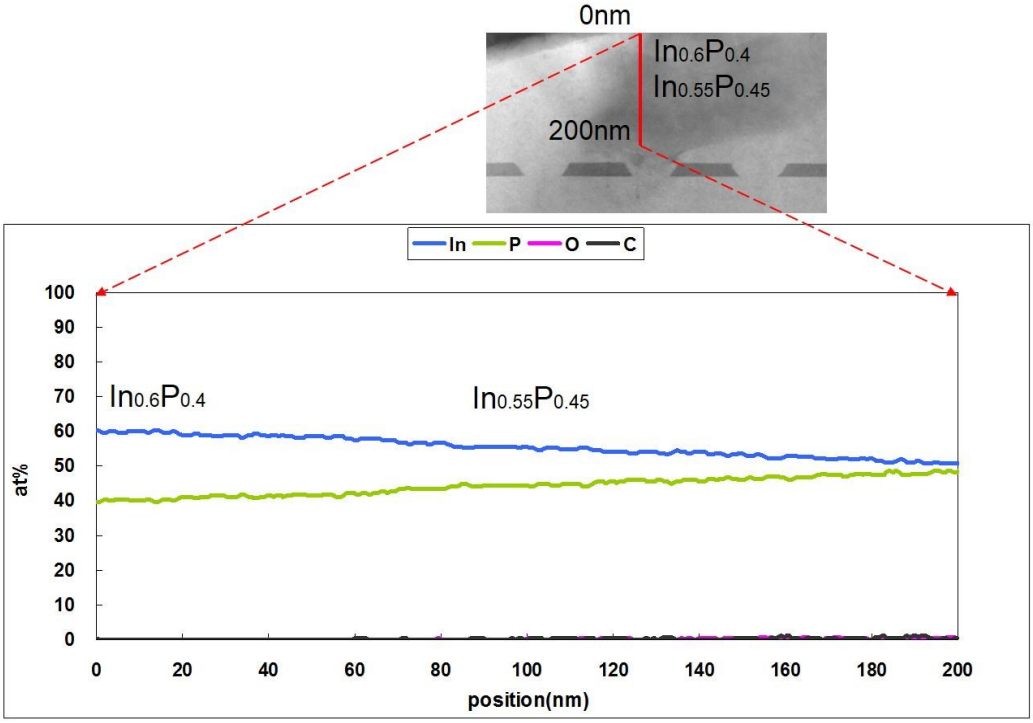

Figure 5. EDS Linescan after the V-Defect Growth Showing the Chemical Composition Gradient in Phosphorus and Indium from the Surface to Bottom. The Upper Region of V-defect Showed More Phosphorus-Deficient and Indium-Rich ($In_{0.6}P_{0.4}$), while the Lower V-defect Showed Less Non-Stoichiometry. At the Linescan Depth of 100nm, the Composition of the Non-Stoichiometric Compound was $In_{0.55}P_{0.45}$

Figure 6 shows the EDS linescan at the upper left portion of V-defect after the growth process. Near the top of the V-defect, the non-stoichiometry was again most pronounced, and the EDS indicated that the compound was $In_{0.55}P_{0.45}$. As the linescan moved deeper from the surface, the ratio of In to P again was decreasing. The EDS linescan suggested that the lower left region of V-defect was nearly a stoichiometric compound of InP.

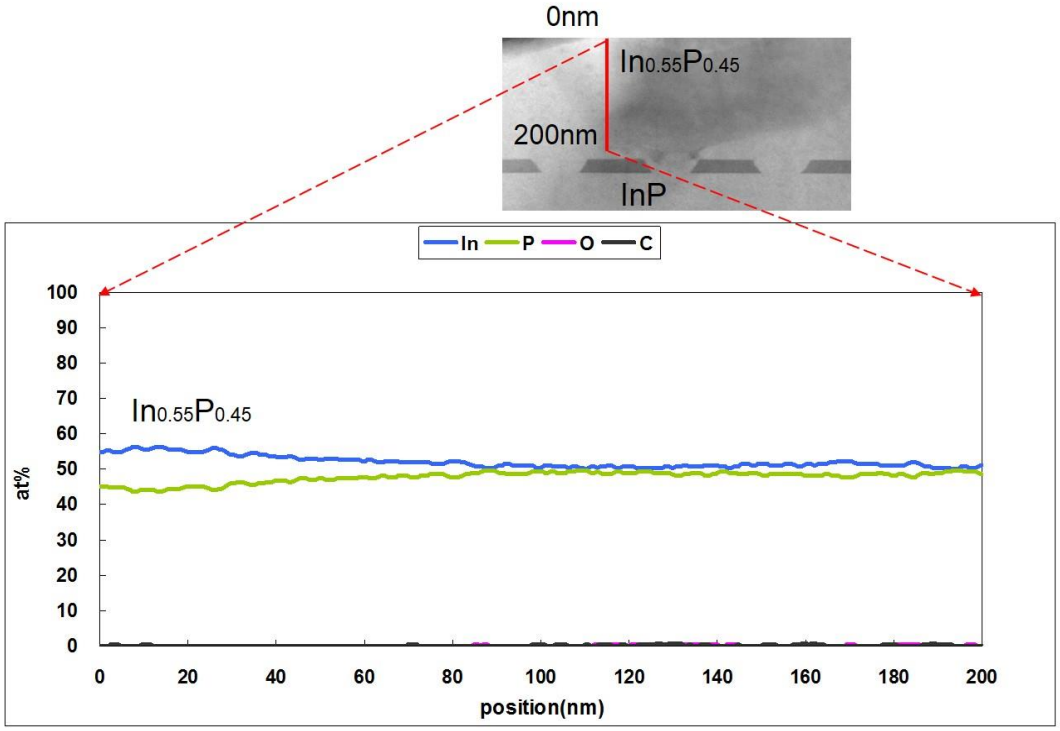

Figure 6. EDS Linescan at the Upper Left Portion of V-Defect after the Growth Process Showing the Chemical Composition Gradient in Phosphorus and Indium from the Surface to Bottom. The Upper Region of V-Defect Showed More Phosphorus-Deficient and Indium-Rich ($In_{0.55}$ $P_{0.45}$), while the Lower V-Defect Showed Less Non-Stoichiometry

4. Discussion

In the following, we attempt to explain the formation mechanism of non-stoichiometric V-shaped defect by nucleation and growth processes.

4.1 Defect Nucleation

The TEM image in Figure 2 suggested that the defect nucleation initiated at the InP groove between the InGaAsP/InP arrays. During the RIE etching, the chlorine-based etching of BCl_3 reacted with the InP to form chlorine-based etch products such as PCl_x. Those chlorine-based etch products have very high volatility that would lead to the preferential loss of phosphorus (Bae et al., 2007). As a result, the phosphorus-deficient region was likely to form along the sidewall and bottom of the groove after the RIE etching, as illustrated in Figure 7. The P-deficient region acted as the nucleation site that played an important role in the subsequent growth of the V-shaped defect.

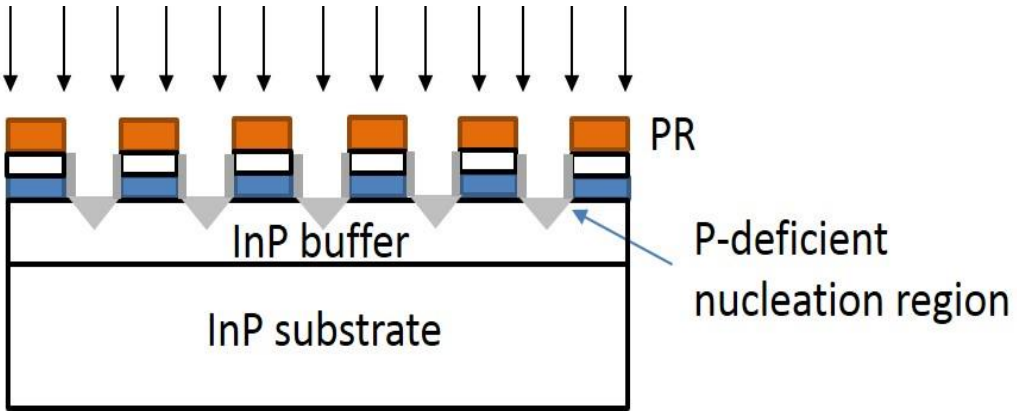

Figure 7. Schematics of V-Defect Nucleation Process. The Nucleation of V-Defect Started at the Groove of the InGaAsP/InP Heterogeneous Array

4.2 Defect Growth

The TEM and EDS data in Figures 3-6 indicated that V-defect was an open, inverted pyramid shape with non-stoichiometric In and P ratio. Moreover, there was concentration gradient in the non-stoichiometric V-defect where the ratio of In to P was decreasing from the top to the bottom and from the center to the side.

Figure 8 shows the schematic of the V-defect growth process. After forming the phosphorus-deficient nucleation seed at the groove, the non-stoichiometric compound continued to grow with the InP regrowth layer. We speculated that the driving force of the P-deficient, In-rich compound growth was related to the reduction of surface energy (Tu et al., 1996). The P-deficient, In-rich ($In_{1+x}P_{1-x}$) compound grew into V-shape to reach the lowest surface energy. The boundary of the V-shaped defect was likely following the crystallographic plane. We also noted that the V-defect formation only preferentially occurred at certain sites. The defect nuclei at those sites have likely reached the "threshold" for the defect growth to occur.

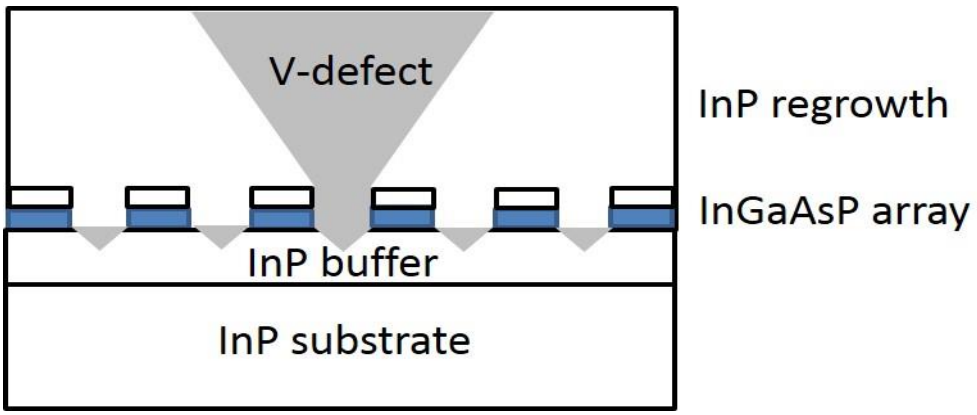

Figure 8. Schematics of V-Defect Growth Process. The Growth of V-Defect Initiated from the Nucleation at the Groove and Expanded to the Surface

The characterization of the P-deficient, In-rich compound in this study may lead to several useful technological applications. First, unfolding the nucleation process of the V-shaped compound may lead to better defect control. Additionally, the nucleation of the V-shaped defect and its interplay with the epitaxial growth in the InP system are important for the engineering of MOCVD or Molecular Beam Epitaxial (MBE). Second, the size, spacing and stoichiometry of the P-deficient, In-rich compound can be engineering tailored. Our study shows that the size and spacing of the nanoscale V-defect could be defined by the InGaAsP/InP position-controlled seed array. For example, the density of the P-deficient compound can be varied by changing the spacing of the InGaAsP/InP nano-array. The non-stoichiometry and optical property of the disordered $In_{1+x}P_{1-x}$ compound may be adjusted by the thickness of the InP regrowth layer. For example, the Photoluminescence (PL) Full-Width at Half Maximum (FWHM) could be reduced as the V/III ratio is lowered, leading to an improvement in the optical quality (Yoon & Zhang, 1998).

5. Conclusion

We have studied the nanoscale nucleation and growth of V-shaped defect in the heterogeneous InGaAsP/InP array with 100nm spacing. We showed that the nucleation originated from the phosphorus-deficient disordering, likely induced by reactive ion etching. The phosphorus-deficient, indium-rich compound ($In_{1+x}P_{1-x}$) was also associated with the triangular nano-precipitates with sizes of 20-30nm, located adjacent to the InP cap. The ratio of In to P in the non-stoichiometric compound was increasing from the bottom to the upper portion of the V-defect likely due to antisite defect mechanism. During the defect growth process, certain phosphorus-deficient nucleation sites expanded to form open, inverted pyramid V-defects with sidewalls following the crystallographic planes.

Acknowledgment

The authors would like to thank MA-Tek (Hsinchu, Taiwan) for their assistance in TEM sample preparation.

References

Bae, J. W., Jeong, C. H., Lim, J. T., Lee, H. C., Yeom, G. Y., & Adesida, I. (2007). Anisotropic etching of InP and InGaAs by using an inductively coupled plasma in Cl_2/N_2 and Cl_2/Ar mixtures at low bias power. *J. Korean Phys. Soc.*, *50*(4), 1130-1135. https://doi.org/10.3938/jkps.50.1130

Bowers, J. E., Ramaswamy, A., Dai, D., Zaoui, W. S., Kang, Y., Yin, T., & Morse, M. (2010). Recent advances in Ge/Si PIN and APD photodetectors. *Physica Status Solidi C*, *7*(10), 2526-2531. https://doi.org/10.1002/pssc.200983875

Charlier, J.-C. (2002). Defects in carbon nanotubes. *Accouts of Chemical Research*, *35*(12), 1063-1069. https://doi.org/10.1021/ar010166k

Chen, Y., Takeuchi, T., Amano, H., Akasaki, I., Yamada, N., Kaneko, Y., & Wang, S. Y. (1998). Pit

formation in GaInN quantum wells. *Applied Physics Letters*, *72*(6), 710-712. https://doi.org/10.1063/1.120853

Collins, P. G. (2009). *Defects and disorder in carbon nanotubes. Oxford Handbook of Nanoscience and Technology: Frontiers and Advances* (A. V. Narlikar, & Y. Y. Fu, Eds.). Oxford: Oxford Univ. Press.

Dregely, D., Taubert, R., Dorfmüller, J., Vogelgesang, R., Kern, K., & Giessen, H. (2011). 3D optical Yagi-Uda nanoantenna array. *Nature Communications*, *2*(267), 1-7. https://doi.org/10.1038/ncomms1268

Drexler, K. E. (1986). *Engines of creation: The coming era of nanotechnology*. New York, NY: Anchor Books.

Duan, X., Huang, Y., Agarwal, R., & Lieber, C. M. (2003). Single-nanowire electrically driven lasers. *Nature*, *421*, 241-245. https://doi.org/10.1038/nature01353

Duan, X., Huang, Y., Cui, Y., Wang, J., & Lieber, C. M. (2001). Indium phosphide nanowires as building blocks for nanoscale electronic and optoelectronic devices. *Nature*, *409*, 66-69. https://doi.org/10.1038/35051047

Fan, Y., Goldsmith, B. R., & Collins, P. G. (2005). Identifying and counting point defects in carbon nanotubes. *Nature Materials*, *4*(12), 906-911. https://doi.org/10.1038/nmat1516

Feynman, R. P. (1992). There is plenty of room at the bottom. *Journal Microelectromechanical Systems*, *1*(1), 60-66. https://doi.org/10.1109/84.128057

Giannuzzi, L. A., Drown, J. L., Brown, S. R., Irwin, R. B., & Stevie, F. A. (1997). Preparation of transmission electron microscopy cross-section specimens using focused ion beam milling, *Materials Research Society Symposium Proceedings*, *480*, 19.

Giannuzzi, L. A., Kempshall, B. W., Schwarz, S. M., Lomness, J. K., Prenitzer, B. I., & Stevie, F. A. (2010). *FIB lift-out specimen preparation techniques ex-Situ and in-Situ methods. Introduction to focused ion beams: Instrumentation, theory, techniques and practice* (Chapter 10, pp. 201-228). New York, NY: Springer.

Gilfert, C., Pavelescu, E.-M., & Reithmaier, J. P. (2010). Influence of the As2/As4 growth modes on the formation of quantum dot-like InAs islands grown on InAlGaAs/InP (100). *Applied Physics Letters*, *96*(191903), 1-3. https://doi.org/10.1063/1.3428956

Huang, J. S., Vartuli, C. B., Nguyen, T., Bar-Chaim, N., Shearer, J., Fisher, C., & Anderson, S. (2002). Correlation of resistance and interfacial reaction of contacts to n-type InP. *Journal of Materials Research*, *17*(11), 2929-2934. https://doi.org/10.1557/JMR.2002.0424

Kim, I. H., Park, H. S., Park, Y. J., & Kim, T. (1998). Formation of V-shaped pits in InGaN/GaN multiquantum wells and bulk InGaN films. *Applied Physics Letters*, *73*(12), 1634-1636. https://doi.org/10.1063/1.122229

Korgel, B. A. (2006). Semiconductor nanowires: Twins cause kinks. *Nature Materials*, *5*, 521-522. https://doi.org/10.1038/nmat1688

Mattila, T., & Nieminen, R. M. (1995). Direct antisite formation in electron irradiation of GaAs. *Physical Review Letters*, *74*(14), 2721-2724. https://doi.org/10.1103/PhysRevLett.74.2721

Narayan, R. J., Kumta, P. N., Sfeir, C., Lee, D.-H., Choi, D., & Olton, D. (2004). Nanostructured Ceramics in Medical Devices: Applications and Prospects. *Journal of The Minerals, Metals & Materials Society*, *56*(10), 38-43. https://doi.org/10.1007/s11837-004-0289-x

Paull, J., & Lyons, K. (2008). Nanotechnology: The Next Challenge for Organics. *Journal Organic Systems*, *3*(1), 3-22.

Regan, B. C., Aloni, S., Jensen, K., Ritchie, R. O., & Zettl, A. (2005). Nanocrystal-Powered Nanomotor. *Nano Letters*, *5*(9), 1730-1733. https://doi.org/10.1021/nl0510659

Saini, R., Saini, S., & Sharma, S. (2010). Nanotechnology: The Future Medicine. *Journal of Cutaneous and Aesthetic Surgery*, *3*(1), 32-33. https://doi.org/10.4103/0974-2077.63301

Seitsonen, A. P., Virkkunen, R., Puska, M. J., & Nieminen, R. M. (1994). Indium and phosphorus vacancies and antisites in InP. *Phys. Rev. B.*, *49*(8), 5253-5262. https://doi.org/10.1103/PhysRevB.49.5253

Sharma, N., Thomas, P., Tricker, D., & Humphreys, C. (2000), Chemical mapping and formation of V-defects in InGaN multiple quantum wells. *Applied Physics Letters*, *77*(9), 1274-1276. https://doi.org/10.1063/1.1289904

Sidiropoulos, P. H., Röder, R., Geburt, S., Hess, O., Maier, S. A., Ronning, C., & Oulton, R. F. (2014). Ultrafast plasmonic nanowire lasers near the surface plasmon frequency. *Nature Physics*, *10*, 870-876. https://doi.org/10.1038/nphys3103

Tham, D., Nam, C., & Fischer, J. E. (2006). Defects in GaN Nanowires. *Advanced Functional Materials*, *16*(9), 1197-1202. https://doi.org/10.1002/adfm.200500807

Tu, K. N., Mayer, J. W., & Feldman, L. C. (1996). *Electronic Thin Film Science for Electrical Engineering and Materials Scientists*. Macmillan, New York, NY.

Wang, R. P. (2006). Defects in silicon nanowires. *Applied Physics Letters*, *88*, 142104-142106. https://doi.org/10.1063/1.2191830

Wu, X. H., Elsass, C. R., Abare, A., Mack, M., Keller, S., Petroff, P. M., & Rosner, S. J. (1998). Structural origin of V-defects and correlation with localized excitonic centers in InGaN/GaN multiple quantum wells. *Applied Physics. Letters*, *72*(6), 692-694. https://doi.org/10.1063/1.120844

Yoon, S. F., & Zhang, H. Q. (1998). Characteristics of InP epitaxial layers grown from solid phosphorus using a valve phosphorus cracker cell. *Optical Materials*, *10*(3), 219-224. https://doi.org/10.1016/S0925-3467(97)00179-1